ADVANCED FUNCTIONAL MATERIALS
www.afm-journal.de

From Membrane to Skin: Aqueous Permeation Control Through Light-Responsive Amphiphilic Polymer Co-Networks

Katrin Schöller, Sabrina Küpfer, Lukas Baumann, Patrick M. Hoyer, Damien de Courten, René M. Rossi, Aliaksei Vetushka, Martin Wolf, Nico Bruns, and Lukas J. Scherer**

The functionalization of amphiphilic polymer co-networks with light-responsive spiropyran and spirooxazine derivatives leads to a new type of light-responsive materials. The material consisting of hydrophilic nano-channels shows desirable properties such as light-responsive permeability changes of aqueous caffeine solutions, an exceptional repeatability of the photochromism, and tunable basic permeability rates. The versatility of the system is demonstrated by using different functionalization routes such as copolymerization of light-responsive monomers or crosslinker as well as postmodification of the preformed amphiphilic network. Moreover, light-responsive spirobenzopyran and novel spirooxazine derivatives are synthesized, which changes the properties of the light-responsive membranes after inclusion into the amphiphilic co-networks. Finally, the permeability of the delivery membrane can be tailored to match the properties of porcine skin, an in vitro model of human neonatal skin. One possible application might be the use of the light-responsive membranes as key-unit of a transdermal caffeine-delivery system for preterm neonates.

Dr. K. Schöller, S. Küpfer, Dr. L. Baumann,
Dr. R. M. Rossi, Dr. L. J. Scherer
Empa, Swiss Federal Laboratories for Materials Science and Technology
Lerchenfeldstrasse 5, 9014, St. Gallen, Switzerland
E-mail: katrin.schoeller@empa.ch;
Lukas.Scherer@empa.ch

P. M. Hoyer, D. de Courten, Prof. M. Wolf
Division of Neonatology
University Hospital Zurich
Frauenklinikstrasse 10
8091, Zürich, Switzerland

Dr. A. Vetushka
Laboratory for Joining Technologies & Corrosion
Empa, Swiss Federal Laboratories for Materials Science and Technology
Überlandstrasse 129
8600, Dübendorf, Switzerland

Dr. A. Vetushka
Laboratory of Nanostructures and Nanomaterials
Institute of Physics
Academy of Sciences of the Czech Republic
Cukrovarnicka 10, 162 00 Prague 6
Czech Republic

Prof. N. Bruns
Adolphe Merkle Institute
University of Fribourg
Rte de l'Ancienne Papeterie, CP209, 1723 Marly, Switzerland

DOI: 10.1002/adfm.201400671

1. Introduction

Stimuli-responsive materials have found widespread applications, as the need to create novel "smart" systems often requires materials that can change their chemical and/or physical properties by changing an external parameter.[1] In the field of medical materials, one future perspective is to employ adaptive materials that allow the simultaneous monitoring of physiological parameters to deliver drugs "on-demand".[2] One example aiming in this direction is the development of a "smart" or programmable transdermal delivery system for preterm neonates that could overcome peaks in drug concentration generated by oral or venous medication.[3]

Recently developed transdermal delivery techniques for adults that decrease the high permeability resistance of skin (stratum corneum) and allow a controlled continuous or pulsed release are non-applicable here because of the vulnerability of preterm neonates.[3,4] A responsive membrane, which changes its permeability on an external stimulus, could help solving this problem. For applications close to the human body, light is the ideal stimulus because light can be applied rapidly and remotely controlled and can be easily focused on small and defined areas.[5] Most of the available light-responsive membranes are based on porous structures, where the light-responsiveness derives from a change in pore diameter or a change in pore wetting due to changes in the surface tension of the membrane.[6] However, only few light-responsive non-porous membranes based on polymer matrices, such as liquid crystals for gas permeation, are known.[7] Typically employed techniques for introducing light-responsiveness to porous membranes are the covalent surface functionalization by small molecules, surface-induced polymer grafting ("grafting from"), or grafting pre-prepared polymers to the membrane surface.[6–8] For example, plasma induced graft polymerization was employed for the coating of pore walls with photochromic copolymers, as recently demonstrated by our group.[8] Although essential for drug-release systems, an exact tuning of the permeability rate is difficult to perform by methods such as grafting from commercial track-etched membranes due to the limited available types of membranes and several complex production steps.[9]

Natural skin displays characteristics such as a very high permeability resistance, an amphiphilic heterophase structure, and a passive diffusion mechanism for molecules, governed by the solubility and phase distribution in the heteropolar domains.[10] In order to achieve an optimum adaptability and responsive "on-off" behavior of a membrane in contact to skin, our idea was to imitate the amphiphilic properties of the natural skin and additionally render the material stimuli-responsive. Non-responsive amphiphilic polymer membranes were already proposed for imitating the permeability characteristics of skin and as model systems for transdermal release.[10] On the other hand, non-amphiphilic hydrogels are commonly used in transdermal drug-delivery systems,[11] and there are several examples of photoresponsive hydrogels in the literature.[12] To obtain photochromic polymers, chromophores such as azobenzenes, dithienylethenes, spiropyrans, and spirooxazines have been integrated into the materials.[5] However, a polymer membrane that is both light-responsive and posseses an amphiphilic heterophase structure has not been reported yet. Therefore, light-responsive, nanostructured amphiphilic membranes where developed by incorporating spirobenzopyrans or spirooxazines in non-porous films of amphiphilic cross-linked copolymers, so-called amphiphilic polymer co-networks (APCNs).[11] APCNs are materials that consist of immiscible hydrophilic and hydrophobic polymer chains. Covalent cross-linking of the chains prevents the macroscopic demixing of the polymers. Instead, phase separated morphologies with domain-sizes on the nanoscale are formed.[12] APCNs swell in water and are therefore a class of hydrogels. In contrast to typical hydrogels, however, APCNs possess drastically improved mechanical stability,[11] which is an essential requirement when used as membrane.[12a,c,13] In addition, characteristics such as biocompatibility, biostability, high oxygen permeability, and their nanophase separated, co-continuous morphologies[11] make them appealing for the application as controlled drug release matrices,[14] as contact lenses,[15] cell culture surfaces,[16] tissue engineering scaffolds,[17] immunoisolation membranes,[18] biomaterials,[19] antifouling surfaces,[20] sensors,[12a] and nanoreactors.[21]

A great advantage of APCNs compared to commercial available porous membranes is that the permeability resistance of the material can be arbitrarily selected by adjusting the composition and the thickness of the membrane. Therefore, the membrane can be tailored to match the permeability of a certain skin type, as will be demonstrated for the delivery of caffeine to a skin model of preterm neonates. Tunable and light-switchable permeation properties of the photochromic APCNs presented herein make them ideally suited as membranes for transdermal delivery devices.

2. Results and Discussion

2.1. Synthesis of Spiropyran (SP) and Spirooxazine (SO) Dyes

Spiropyrans and spirooxazines are known to undergo a reversible heterolytic ring-opening reaction upon UV irradiation leading to a polar and colored merocyanine (MC) state, while illumination with white light results in a ring-closing reaction back into its initial spiropyran (SP) state (see reaction scheme in **Figure 1**).[5]

To produce membranes with light-responsive permeability changes, the membranes were covalently functionalized with different SP and SO based molecules following two strategies. In the first approach, a spiropyran (**SP1**) was synthesized that was conjugated with the hydroxyl groups of the side-chains of the polymer via esterification allowing the postmodification of preformed membranes. In the second approach, polymerizable SP and SO based dyes were synthesized in order to incorporate them into the membranes via copolymerization during the membrane production step. The chemical structures of the synthesized chromophores are shown in **Figure 2** (experimental details in Supporting Information). In addition to the monofunctional spiropyran acrylate (**SP2**), a spirooxazine with two polymerizable groups (**SO1**) was synthesized because of its proposed photostability and to see if a steric impact can be added to the electrostatic response of the chromophores.[22] A steric effect could either enhance or decrease the light-responsive permeability change resulting from the polarity change. A similar concept has been previously presented with the incorporation of an SP containing crosslinker into a polymeric matrix resulting in mechanochromic materials.[23]

2.2. Synthesis of Light-Responsive Amphiphilic Polymer Co-Networks

APCNs consisting of poly(2-hydroxyethyl acrylate) (PHEA) as hydrophilic component and poly(dimethylsiloxane) (PDMS) as hydrophobic component were chosen as base material for the light-responsive membranes, since these APCNs are soft, flexible and elastic at room temperature.[12a] To prevent macroscopic phase separation before or during polymerization, the hydrophilic monomer HEA was initially protected with a non-polar trimethylsilyl (TMS) protecting group. This monomer was copolymerized with a PDMS crosslinker by light-initiated free radical polymerization (**Figure 3**). Membranes with a thickness of 200, 300 and 400 µm, respectively, were prepared. After

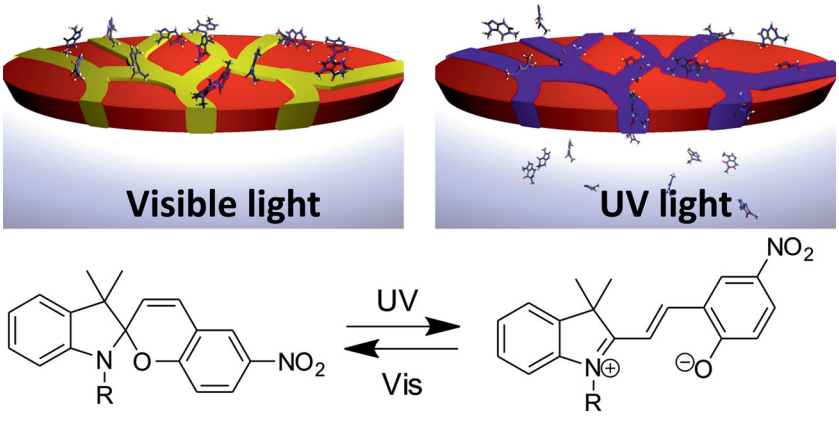

Figure 1. Scheme showing the working principle of light-responsive APCNs. Reversible polarity change from the spiropyran to the merocyanine state in the hydrophilic domains of an APCN results in a change of permeability for aqueous caffeine solutions.

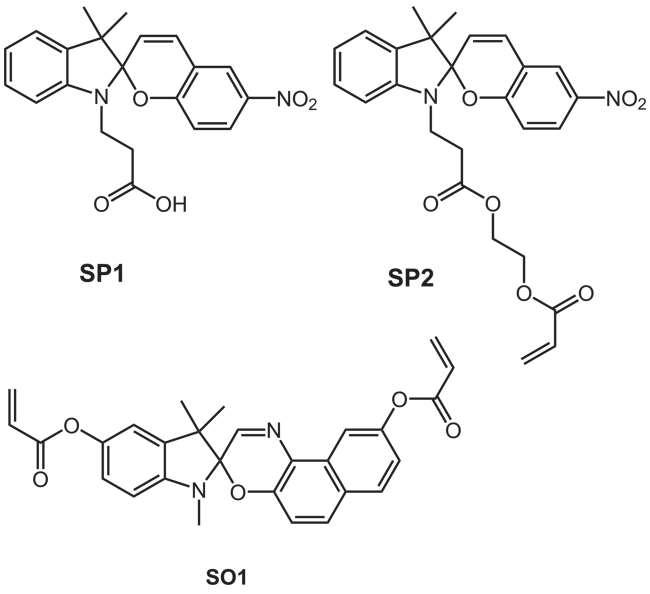

Figure 2. Chemical structures showing the synthesized light-responsive spiropyran and spirooxazine dyes.

the polymerization, the protection group was removed using slightly acidic aqueous conditions. A macroscopic phase separation was not any longer possible due to the covalent crosslinking of the polymer chains resulting in a phase separated morphology with domains in the nanoscale range.

The synthesized dyes were incorporated in APCNs either by postmodification (**SP1**) or copolymerization (**SP2**, **SO1**) (Figure 3). For the postmodification approach, APCNs without dyes were synthesized, followed by esterification of the hydroxyl groups of PHEA's side-chains with the carboxylic acid functionality of **SP1** (Figure 3a). Copolymerization was carried out with 1 wt% of **SP2** (maximum amount of SP2 soluble in the monomer mixture) and 0.4 wt% of **SO1** in the monomer mixture. In all cases three different monomer ratios between the TMS-protected HEA and the PDMS macromonomer were employed, which were 50/50, 60/40, and 70/30. In the following discussion, copolymerized membranes are written as CP X/Y (**SP2** as comonomer) or SO X/Y (**SO1** as comonomer), and the postmodified membranes as PM X/Y, where X/Y describes the ratio between the amounts of TMS-HEA (X) and PDMS (Y) used in the membrane synthesis.

First polymerization attempts showed that it was not possible to initiate the copolymerization with UV light in the presence of **SP2**. This was due to the strong absorption of spiropyran in the UV range, which prevented the photoinitiator from being excited and forming radicals. As a consequence, Irgacure 819 – a photoinitiator creating radicals when irradiated with light in the visible range – was used, and the reaction was initiated with white light. Monomer conversion and deprotection was followed via IR measurements (Figure S3, Supporting Information). Full conversion of monomers was assessed by the absence of absorption bands at 1658, 1403, and 1370 cm^{-1}, which are typical for the C=C double bonds of the monomers.[12a] The successful deprotection of TMS-HEA was confirmed in all measured spectra by the appearance of a broad peak at 3400 cm^{-1} indicating the stretch absorption of the free O-H group.

The postmodified membranes were light-red under daylight. Illumination with white light (400–700 nm, 500 Lumen) led to a complete decoloration. Irradiation with UV-light (386 nm, 1.5 mW cm^{-2}) yielded a strongly red-colored membrane. Copolymerized membranes were slightly red even when irradiated with white light but showed similar behavior under UV-irradiation as the postmodified membranes (Figure 3, right).

2.3. Characterization of Membranes with SP

The membranes were characterized in different ways to prove that the typical characteristics of non-functionalized APCNs were maintained despite the presence of **SP2**. Important characteristics of amphiphilic co-networks are their ability to swell in solvents of opposing polarity, such as water and organic solvents. The volumetric swelling degree *S* was determined for membranes in hexane and water. One can expect that a larger PDMS content would lead to a decreased swelling in water,

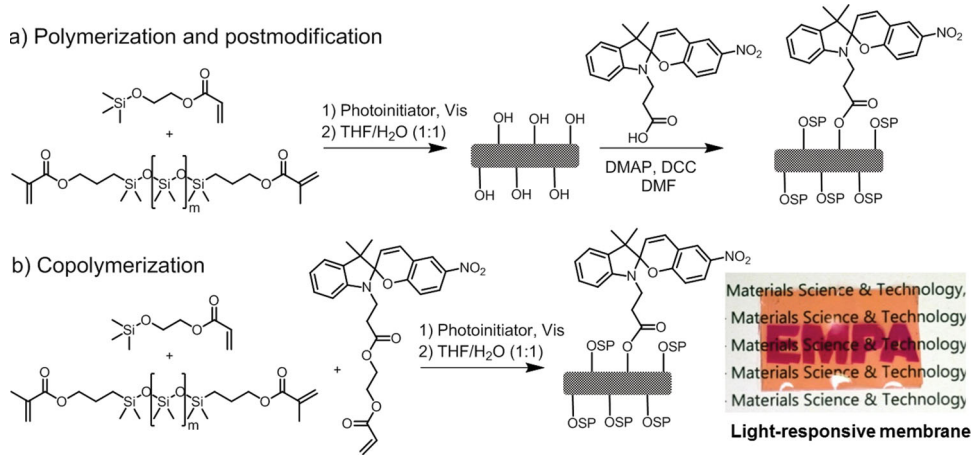

Figure 3. Reaction scheme showing the preparation of light-responsive amphiphilic polymer co-networks via a) polymerization and postmodification and b) copolymerization in bulk, and a photograph of the resulting transparent membrane after partial illumination with UV light.

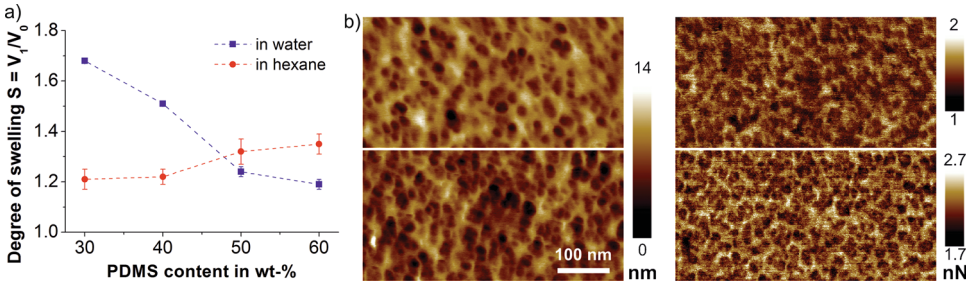

Figure 4. Characterization of light-responsive APCNs prepared via copolymerization with SP2 and different amounts of PDMS and PHEA before UV irradiation. a) Volumetric swelling degree of membranes in water and in hexane. b) AFM peakforce QNM height (left) and adhesion maps (right) of membranes with 30% (upper row) and 50% PDMS (bottom row). The bright domains correspond to the PHEA phase and the dark regions to the PDMS phase.

whereas the swelling in hexane would increase.[24] In **Figure 4**a it can be seen that the swelling behavior followed the expected trends. Moreover, the irradiation with UV light had no influence on the swelling behavior of a given membrane (Table S1, Supporting Information). Because the amount of spiropyran in the membrane was rather small, consequently changes in the swelling behavior were most likely too small to be detected.

Peak force atomic force microscopy (AFM) height maps and adhesion maps of the membranes reveal a nanophase separated morphology as it is typical for APCNs (Figure 4b). The bright phase is assumed to be PHEA whereas the dark phase is assumed to correlate with PDMS.[24] From AFM measurements disclosed for two membranes (CP70/30 and CP50/50), a domain size of the PDMS-phase between 20–50 nm can be determined. Similar to non-functionalized APCNs, the PHEA phase displays an interconnected structure in both cases, whereas the PDMS domains form an island-like structure that becomes more and more interconnected with increasing PDMS content. The adhesion images confirm the interconnected structure of the PHEA domains, showing higher values of adhesion for the PHEA phase as compared to the PDMS phase, which is in agreement with its suggested hydrophilic behavior.

The total area of the PDMS vs. the PHEA phase on the surface of the membranes, calculated from black and white images, increases remarkably with increasing PDMS content (Figure S4, Supporting Information). Postmodified as well as copolymerized membranes showed similar IR spectra for the surface and the bulk (Figure S3, Supporting Information). Therefore, it was concluded that PHEA as well as PDMS were present in a similar ratio at the surface and in the bulk of the membranes, i.e., none of the monomers accumulated on the surface during curing of the monomer mixture.

2.4. Reversibility of Photochromic Switching and Decoloration Kinetics

To gain more insight into the light-responsive properties and their relation to the permeability of the membranes, UV-Vis measurements were performed. At first the reversible photochromic switching of the incorporated spiropyrans from the colorless, non-polar SP state to the colored, polar MC form was analyzed. The photochromic switching also changed the permeability of the membranes, which is discussed in more detail in the next section. **Figure 5**a shows the reversible photochromic switching of a postmodified SP-containing membrane 15 times by alternately illuminating the membrane for 15 s with UV and white light. For all types of membranes with SP reported here, more than 75 times switching was possible (Figure 5b and Figure S5, Supporting Information). The difference in transmission between the MC and SP form after 75 cycles remains 54% of that of the first cycle for PM 60/40 and 29% for CP 50/50. This is relatively high for a spiropyran based polymeric material, as photodegradation of the MC form in UV light is a well-known problem for spiropyran based photochromic systems.[22,25] For example, the difference in transmission of the

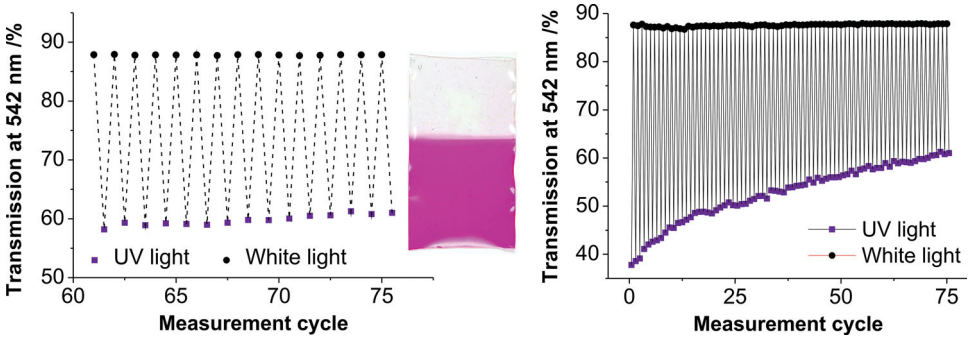

Figure 5. Reversibility of color switching between the spiropyran (colorless/transparent) and the merocyanine (purple) state in a membrane (PM 60/40) measured at 542 nm at sequential illumination with UV and white light for 15 s: cycle 51–76 (left) and cycle 1–76 (right). The inset in the left diagram shows a postmodified membrane in its colorless (upper part) and colored state (lower part).

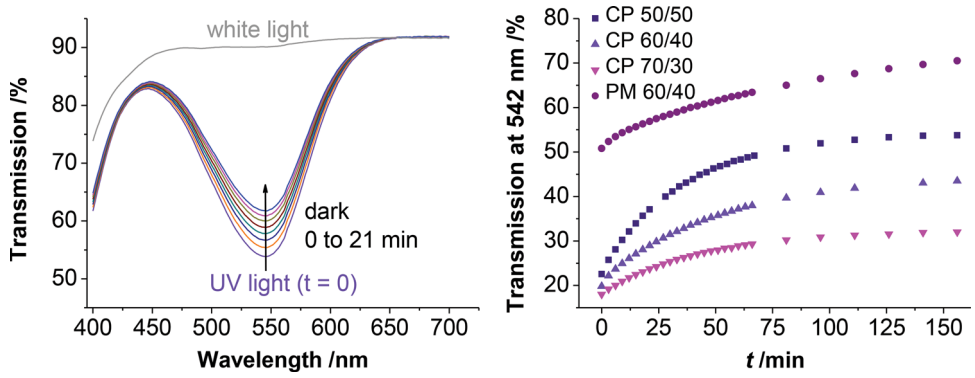

Figure 6. Transmission spectra of a membrane (PM 60/40) after UV irradiation and additional storage in the dark (left); transmission at 542 nm of SP containing APCNs with different PDMS/PHEA ratios (right), each after UV illumination for 1 min, measured at different time intervals in the dark (decoloration kinetics).

25th cycle is still 75% of that of the first cycle for PM 60/40, while in similar polymeric systems with covalently bound spiropyran molecules, changes of comparable dimensions were already observed after 12 switching cycles.[26]

A high photostability of spiropyrans in combination with a slow ring-closing reaction from the MC to the SP state would allow the use of pulsed UV-irradiation for release or sensing applications. This could increase the operational life span of a photochromic membrane remarkably. Therefore, the ring-closing kinetics of the MC form towards the SP form within APCNs was determined by measuring the decoloration kinetics in dark conditions. For all SP containing membranes, the initial decoloration rate after UV-illumination for 1 min slowed down at first and reached a plateau after about one hour (**Figure 6**). After 18 min the difference in transmission between the MC and SP form is still more than 85% of its original value for PM 60/40, which demonstrates that the ring-closing reaction is slow enough to allow for a release of caffeine by pulsed UV irradiation. Comparison of the decoloration kinetics of SP in copolymerized membranes with varying PHEA/PDMS ratio shows, that with increasing PDMS content the decoloration was accelerated. Additionally, comparison of copolymerized and postmodified membranes displayed that the decoloration was generally slower for postmodified membranes (Figure 6). The different photochromic behavior of copolymerized and postmodified membranes was probably due to a different environment of the chromophore on the nanoscale. From the literature it is known that the chemical environment of the SP molecules has a major influence on the speed of the decoloration reaction in the dark, and that a more hydrophilic surrounding stabilizes the open merocyanine form.[5,27] The impact of different surroundings of the SP moieties is additionally indicated by the different color of the copolymerized and postmodified membranes in daylight (slightly red vs. colorless, Figure 3 and 5), which hints towards a shifted equilibrium of the reversible photoisomerization in daylight.

The plateau region in the reversibility as well as the decoloration studies implies that an even higher number of switching cycles or even longer times of the colored state are feasible in an application like sensing or drug-delivery, where either a higher number of switching cycles or a longer period of the colored state is desired. Moreover, combining the results of the reversibility and decoloration studies of the postmodified membrane (PM 60/40) shows that, for example, 25 switching cycles with a repeated pulse after 18 min each can be achieved with less than 36% loss in transmission difference between the MC and SP state. In summary, it can be stated that the photostability of the membrane is high enough to allow a device to be operated for 7.5 h in the colored state before an exchange of the membrane is required, which is typically long enough for a transdermal release application.[4b]

2.5. Permeation Properties

The permeability of the membranes is the most important characteristic for a possible application in drug delivery. Caffeine was used in the permeability studies because one possible application of the light-responsive membrane is the continuous transdermal delivery of caffeine in preterm neonates. Applying caffeine to preterm neonates has been demonstrated to decrease the risk of apnea by stimulating the respiratory system and is therefore routinely carried out in hospital.[28] In preterm neonates the stratum corneum is not developed yet during the first days after birth, therefore their skin is more permeable than that of adults. This eases the transdermal drug delivery.[29]

For non-amphiphilic hydrogels a dependence of the polarity of the network on the permeability due to swelling and/or change in the interaction between the solute and the polymer matrix (partition mechanism) was demonstrated.[10,24,30] The diffusion of caffeine molecules through the hydrophilic channels of APCNs is governed by the swelling and polarity of the polymer network. Therefore, the aim was to modify the polarity of the membrane by transforming spirobenzopyran or spirooxazine from the open to the closed state and vice versa. Because the merocyanine form of the molecule is charged, it is more hydrophilic than in the closed SP form. This would lead to an increased permeability or increased molecular flux of caffeine (F) through the membrane if the chromophores are in their merocyanine form.[8] To tune the basic permeability of the membrane, the thickness and the ratio of HEA and PDMS of the networks were varied. All membranes were measured under white light and under UV light and the resulting average flux of caffeine is summarized in **Figure 7**.

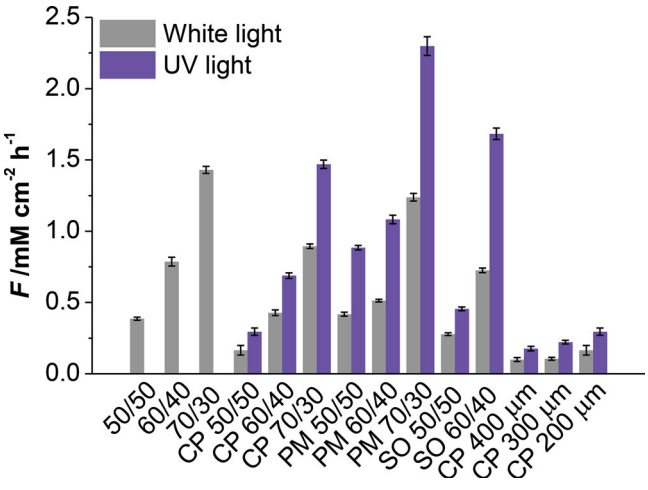

Figure 7. Average flux *F* of aqueous caffeine (93 mM) for different APCNs (200 µm thick, unless otherwise noted) after irradiation with white or UV light, the difference in *F* between white light and UV irradiation shows the permeability switch between the two states.

In general, it was found that the average flux could be tuned between 0.1 and 1.4 mM cm^{-2} h^{-1} by changing either the thickness or the PHEA/PDMS ratio of the membranes. The more PHEA the network contained, the higher the average molecular flux through the membrane was. Furthermore, for all dye containing membranes a pronounced increase of permeability was found when the membranes were irradiated with UV light. It is noteworthy that the incorporation of SP in the copolymerized membranes decreased the permeability of the membranes as compared to the membranes without SP. Although this could be another possibility to control the basic permeability, in our study all copolymerized membranes contained the same amount of spirobenzopyran. This way, the basic permeability could be controlled by only changing the composition and thickness of the membrane keeping the permeability switch in the presence of UV light at a maximum value. When irradiated with UV light, the permeability increases to 140% of its original value for the copolymerized membranes and to 150% of its original value in the case of postmodified membranes. This 1.5 fold permeability change is remarkable considering that the APCNs were doped with only 1% **SP2** and the change from the SP to MC state changed the permeability without macroscopically changing the membrane structure (e.g., by swelling).

For the incorporation of **SO1** in the APCNs two effects were assumed: on the one hand a higher stability towards photobleaching[22] and on the other hand it was expected that the bifunctional monomeric structure of SO would lead to an additional crosslinking of the hydrophilic PHEA-phase. We assumed that the combination of the polarity change and the mechanical contracting/dilation effect under UV light – caused by the different distances between the two acrylate units of the SO and the merocyanine form – would lead to an increased change of permeability. Indeed, for the 40% PDMS containing SO-functionalized membranes the highest permeability increase of 157% of its original value was found. Although an increased stability towards photobleaching was expected for SO as compared to SP, in our system the stability in water was decreased after the storage of the membranes for several days. Therefore, SP-functionalized membranes were employed for the comparison to the in vitro skin model.

2.6. Tailoring of APCN Properties to an In-Vitro Skin Model

To enable the continuous permeation of an aqueous caffeine solution from the light-responsive membrane through a given skin, it is necessary to switch the permeability of the membrane from a higher permeability to a lower permeability compared to the permeability of the skin. Therefore, the permeability of skin had to be determined first. In order to simulate the permeability of human preterm neonatal skin, porcine ear skin was chosen due to its physiological similarities to human skin[29] and its high quality to simulate human skin[31] and human preterm neonatal skin.[32] Furthermore, there was no ethical issue because these animal tissue samples are waste-products in slaughterhouses. In contrast to adult skin, the superficial skin layer (stratum corneum layer) in preterm neonates is not yet completely developed. Therefore, the stratum corneum of the porcine skin of adult individuals had to be thinned in order to correctly simulate preterm neonate skin. The adhesive tape-stripping technique was chosen because it is a well-established way to simulate human preterm skin.[31,32] This technique allowed to thin the stratum corneum of porcine ear skin by stripping a defined number of times with the aim to retain just a few layers of stratum corneum.

The flux of aqueous caffeine through the resulting stratum corneum layer of porcine ear skin was determined to be 0.15 mM cm^{-2} h^{-1}, using a standard Franz cell setup.[9] As discussed above, the permeability of APCNs can be tuned by the PHEA-to-PDMS ratio. Figure 7 shows that the investigated APCNs had permeabilities above the value of the preterm neonate skin model. Therefore, APCN CP50/50, the membrane with the lowest permeability in the non-UV irradiated state, was selected and its permeability was further decreased by increasing its thickness from 200 µm to 300 µm (CP 300 µm) and 400 µm (CP 400 µm, Figure 7). The caffeine flux through this membrane under Vis and UV light was then compared with the flux through the thinned stratum corneum of the pig ear skin (**Figure 8**). A 1.5 fold change in caffeine flux, when switched from visible to UV light, was found for the membrane, and the caffeine flux from the in vitro skin model lied exactly between the two permeability states of the membrane. In this way a switching from a state of no or minimum release, where the membrane was less permeable than the skin, to an UV-activated state of maximum release is possible, where the membrane was more permeable than the skin.

The skin permeability of different samples from one individual does not necessarily differ largely, but gender, race, age, weight, and anatomical region cause different skin permeability.[33] What influences the permeability enormously is the different content of hair follicle mainly depending on the age.[34] Therefore, a transdermal delivery system has to be adaptable to the various permeabilities encountered in patients. The basic permeability of APCNs can be tuned by the material's composition and its thickness. In combination with the large changes in permeability caused by the photochromic switching

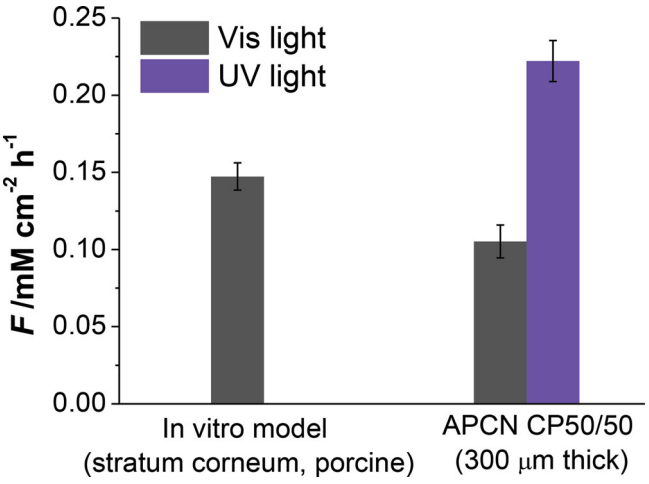

Figure 8. Molecular flux of aqueous caffeine (93 mM) through an SP2 containing APCN (300 μm thick) under UV and Vis light as compared to the caffeine flux through the human preterm neonatal skin model.

of the SP in the APCNs, the materials presented herein could be applicable in transdermal drug delivery devices.

3. Conclusion

In this paper, we demonstrated the incorporation of light-responsive spiropyran- and spirooxazine derivatives into amphiphilic polymer co-networks to create photochromic membranes. The one-step polymerization approach for the preparation of the membranes allowed a covalent binding of chromophores in APCNs and a systematic and simple tuning of membrane characteristics. In addition, the reversibility of color switching and the stability of the colored state were shown with regard to applications in non-invasive drug delivery. The possibility to adjust the permeability as well as a pronounced, up to 1.6 fold permeability change between white and UV light allowed the adjustment of the permeability range to the in vitro preterm neonate skin model. The photochromic APCNs presented here are therefore promising candidates for transdermal drug delivery systems, where a high degree of adaptability and a light-switchable permeability change is desired. Moreover, being flexible with regard to composition and incorporation of functional molecules, these photoresponsive membranes open new doors for on-demand transdermal drug delivery systems by combining the photochromic permeability switching with sensing functionalities in the future.

4. Experimental Section

Materials: Microscope glass slides from Thermo Scientific were used as support and cover for the membrane production. Self-adhesive tape (Tesafilm universal, transparent) was used as spacer unit between the two glass slides. 2-((trimethylsilyl)oxy)ethyl acrylate (TMS-HEA) and α,ω-methacryloxypropyl poly(dimethylsiloxane) (PDMS, 48 to 75 monomer units) were purchased from ABCR. TMS-HEA was distilled under reduced pressure before usage and stored in the freezer for no more than one month. Irgacure 819 was provided by BASF. N,N-Dicyclohexylcarbodiimide (DCC), dimethyl aminopyridine (DMAP), *tert*-butylmethylether (TBME) and 2-butanone were obtained from Sigma Aldrich. Hexane (Hx) was obtained from Biosolve. Tetrahydrofuran (THF) was purchased from Fisher Chemicals. Caffeine and N,N-dimethylformamid (DMF) were purchased from Fluka. All chemicals, unless stated otherwise, were used as delivered without further purification. Distilled water from the in-house supply was used unless stated otherwise.

Synthesis of APCNs: The thickness of the membrane was adjusted by the number of tesa film stripes which were stuck on each other as spacers. Each stripe was about 50 μm thick. Since the spacer was built of up to four to eight layers of tape, membranes with a thickness of 200 μm (if not otherwise stated), 300 μm, or 400 μm were formed. Three different weight ratios (50/50, 60/40, and 70/30 wt%, written as 50/50, 60/40, and 70/30 in the text) of TMS-HEA to PDMS were used to produce membranes and in total 0.625 g monomer mixture was used per membrane. After premixing of TMS-HEA with **SP2** (6.25 mg, 0.013 mmol) or **SO1** (2.5 mg, 0.005 mmol) in the case of networks with SP/SO, the corresponding amount of PDMS was added and shaken vigorously for 1 min. Under red light, Irgacure 819 (5 mg, 0.01 mmol) was added and the mixture was again shaken vigorously for 5 min. The prepared supporting glass slide was generously soused with monomer solution. Then the system was covered with a second glass and irradiated for 20 min from each side with white light (500 W bulb). Subsequently, the slides were dunked into a mixture of THF and water (50/50 vol%) and after 12 h, the membrane was removed from the glass slides and stored in water.

Post-Modification: A round-bottom flask was equipped with a stirrer and a protecting grid. **SP1** (50 mg, 0.27 mmol), DCC (55 mg, 0.27 mmol), DMAP (16 mg, 0.14 mmol), and 40 mL DMF were added to the flask under dry conditions. A membrane without SP that had been stored in DMF for at least 2 h was added and the whole mixture was gently stirred at room temperature for 12 h. The membranes were washed with and stored in distilled water.

Swelling of Membranes: All dimensions were callipered with an *Antichoc 05.10008* from Tesa. A membrane was dried in the desiccator over molecular sieves for one day. Afterwards, its volume (V_0) was determined by measuring the side lengths and the thickness. Then the membrane was placed into water or hexane for 1 h and the volume (V_1) was measured again. For measuring the impact of the MC state on the swelling behavior, a membrane was illuminated with UV-light (366 nm, 8 mW cm^{-2}) for 1 min before swelling in water. Each measurement was repeated three times. The volumetric degree of swelling S was calculated using the following formula:

$$S = \frac{V_1}{V_0} \quad (1)$$

Peak Force QNM Measurements: The samples were measured by a Bruker Icon AFM using silicon Nanoscience Aspire CFMR cantilevers with a force constant of ±3 N m^{-1}, and a resonant frequency of ±75 kHz. The radius of a new tip was ±8 nm. The set point of the Peak Force applied during the measurements was in the range of a few nN, the Peak Force frequency was 2 kHz. The cantilever was calibrated on a Bruker PDMS-SOFT-2-12M test sample (nominal elastic modulus was 3.5 MPa). The scanning speed ranged from 600 to 1000 nm s^{-1}. All AFM measurements were performed at 25 °C and approx. 30% humidity of the ambient air.

Solid State UV-Vis Measurements: All measurements were performed on a Lambda 9 spectrometer (Perkin Elmer) in the transmission mode. The UV irradiation was carried out with a UV-light source (intraLED UV Volpi, 386 nm, 1.5 mW cm^{-2}), the white light source was a intraLED 3 from Volpi (400–700 nm, 500 lumen). After illuminating the membrane for 1 min with UV light, the spectrum of the membrane was measured and the maximal absorbance was detected. The reversibility of the photochromic switch was measured by alternating illumination with UV light and white light (each time illuminated for 15 s with UV and white light, respectively) and the transmission measurement was carried out at the assigned absorption maximum. To obtain information about ring-closing kinetics of the spiro-compounds under dark conditions, first the membrane was illuminated with UV light (1 min), then the transmission at the assigned maximum was measured over a time span of 160 min at room temperature.

Permeability Measurements: All measurements were performed in a Franz diffusion-cell (SES Analysesysteme, receptor volume 12.0 mL and orifice area 1.77 cm^2). Before placing the membranes in the Franz cell, they were either irradiated with UV light (366 nm, 8 mW cm^{-2}) or white light (400–700 nm, 500 Lumen) for 1 min. Mass transfer rates of caffeine were measured under UV irradiation (366 nm, 8 mW cm^{-2}) and at daylight. After filling the receptor chamber with water (12.0 mL), the membrane was fixed in the diffusion cell. The donor chamber was charged with a caffeine solution (93 mM; 3.0 mL). Samples (200 µL) were collected from the receptor part of the cell, typically after 1, 15, 30, 45 min and 1, 1.5, 2, 2.5, 3, 4, 5, 6, 7, 8 h. The caffeine concentrations of these samples were assigned by measuring its UV absorption at 293 nm (calibration curve: $c_{aff} = (0.9068x + 0.0212)$ mMol/L, x: measured absorption). The permeability of a membrane at a given caffeine concentration is proportional to the molecular flux F of aqueous caffeine through the membrane, calculated according to

$$F = \frac{n}{At} \tag{2}$$

where n represents the amount of material per area (A) and per time (t) that diffuses through a membrane. Each value for F was stated with its standard error of the regression coefficient. All membranes were stored in water to precondition the membranes for the permeability measurements. To ensure that the mass transport did not occur through cracks or holes in the membranes but only through the hydrophilic channels, a test with an aqueous dye solution (Bemacid Blue E-2R from Bezema) was once performed for each type of membrane.

Supporting Information

Supporting Information is available from the Wiley Online Library or from the author.

Acknowledgements

This work was financially supported by the Swiss National Science Foundation (NRP 62 – Smart Materials). The AFM studies were supported by Project 14-37427G of the Czech Science Foundation. The support of B. Leuthold, K. Kehl, D. Marti, P. Rupper, U. Bünter, D. Rentsch and M. Rother is gratefully acknowledged.

Received: February 27, 2014
Revised: April 2, 2014
Published online: May 30, 2014

[1] a) M. A. C. Stuart, W. T. S. Huck, J. Genzer, M. Müller, C. Ober, M. Stamm, G. B. Sukhorukov, I. Szleifer, V. V. Tsukruk, M. Urban, F. Winnik, S. Zauscher, I. Luzinov, S. Minko, *Nat. Mater.* **2010**, *9*, 101; b) I. Tokarev, S. Minko, *Adv. Mater.* **2009**, *21*, 241; c) Z. Liu, F. Luo, X.-J. Ju, R. Xie, T. Luo, Y.-M. Sun, L.-Y. Chu, *Adv. Funct. Mater.* **2012**, *22*, 4742.

[2] a) D. F. Stamatialis, B. J. Papenburg, M. Gironés, S. Saiful, S. N. M. Bettahalli, S. Schmitmeier, M. Wessling, *J. Membr. Sci.* **2008**, *308*, 1; b) D. A. LaVan, T. McGuire, R. Langer, *Nat. Biotechnol.* **2003**, *21*, 1184.

[3] K. A. Moga, L. R. Bickford, R. D. Geil, S. S. Dunn, A. A. Pandya, Y. Wang, J. H. Fain, C. F. Archuleta, A. T. O'Neill, J. M. DeSimone, *Adv. Mater.* **2013**, *25*, 5060.

[4] a) M. R. Prausnitz, *Adv. Drug Delivery Rev.* **1999**, *35*, 61; b) M. R. Prausnitz, R. Langer, *Nat. Biotechnol.* **2008**, *26*, 1261.

[5] F. Ercole, T. P. Davis, R. A. Evans, *Polym. Chem.* **2010**, *1*, 37.

[6] F. P. Nicoletta, D. Cupelli, P. Formoso, G. De Filpo, V. Colella, A. Gugliuzza, *Membranes* **2012**, *2*, 134.

[7] E. Głowacki, K. Horovitz, C. W. Tang, K. L. Marshall, *Adv. Funct. Mater.* **2010**, *20*, 2778.

[8] a) L. Baumann, D. de Courten, M. Wolf, R. M. Rossi, L. J. Scherer, *ACS Appl. Mater. Interfaces* **2013**, *5*, 5894; b) L. Baumann, K. Schöller, D. de Courten, D. Marti, M. Frenz, M. Wolf, R. M. Rossi, L. J. Scherer, *RSC Adv.* **2013**, *3*, 23317.

[9] L. Baumann, D. Hegemann, D. de Courten, M. Wolf, R. M. Rossi, W. P. Meier, L. J. Scherer, *Appl. Surf. Sci.* **2013**, *268*, 450.

[10] M. M. Feldstein, I. M. Raigorodskii, A. L. Iordanskii, J. Hadgraft, *J. Controlled Release* **1998**, *52*, 25.

[11] a) C. S. Patrickios, T. K. Georgiou, *Curr. Opin. Colloid Interface Sci.* **2003**, *8*, 76; b) G. Erdodi, J. P. Kennedy, *Prog. Polym. Sci.* **2006**, *31*, 1; c) L. Mespouille, J. L. Hedrick, P. Dubois, *Soft Matter* **2009**, *5*, 4878.

[12] a) M. Hanko, N. Bruns, S. Rentmeister, J. C. Tiller, J. Heinze, *Anal. Chem.* **2006**, *78*, 6376; b) C. Fodor, G. Kali, B. Ivan, *Macromolecules* **2011**, *44*, 4496; c) J. Tobis, L. Boch, Y. Thomann, J. C. Tiller, *J. Membr. Sci.* **2011**, *372*, 219; d) D. Kafouris, M. Gradzielski, C. S. Patrickios, *Macromolecules* **2009**, *42*, 2972.

[13] a) F. E. Du Prez, E. J. Goethals, R. Schué, H. Qariouh, F. Schué, *Polym. Int.* **1998**, *46*, 117; b) X. F. Li, M. Basko, F. Du Prez, I. F. J. Vankelecom, *J. Phys. Chem. B* **2008**, *112*, 16539.

[14] C. P. Lin, I. Gitsov, *Macromolecules* **2010**, *43*, 10017.

[15] P. C. Nicolson, J. Vogt, *Biomaterials* **2001**, *22*, 3273.

[16] A. Haesslein, M. C. Hacker, H. Ueda, D. M. Ammon, R. N. Borazjani, J. F. Kunzler, J. C. Salamone, A. G. Mikos, *J. Biomater. Sci., Polym. Ed.* **2009**, *20*, 49.

[17] Y. Sun, J. Collett, N. J. Fullwood, S. Mac Neil, S. Rimmer, *Biomaterials* **2007**, *28*, 661.

[18] I. S. Isayeva, A. N. Gent, J. P. Kennedy, *J. Polym. Sci., Part A: Polym. Chem.* **2002**, *40*, 2075.

[19] S. K. Jewrajka, G. Erdodi, J. P. Kennedy, D. Ely, G. Dunphy, S. Boehme, F. Popescu, *J. Biomed. Mater. Res., Part A* **2008**, *87A*, 69.

[20] Y. P. Wang, D. E. Betts, J. A. Finlay, L. Brewer, M. E. Callow, J. A. Callow, D. E. Wendt, J. M. DeSimone, *Macromolecules* **2011**, *44*, 878.

[21] N. Bruns, J. C. Tiller, *Nano Lett.* **2005**, *5*, 45.

[22] J. Ratner, N. Kahana, A. Warshawsky, V. Krongauz, *Ind. Eng. Chem. Res.* **1996**, *35*, 1307.

[23] D. A. Davis, A. Hamilton, J. Yang, L. D. Cremar, D. Van Gough, S. L. Potisek, M. T. Ong, P. V. Braun, T. J. Martinez, S. R. White, J. S. Moore, N. R. Sottos, *Nature* **2009**, *459*, 68.

[24] N. Bruns, J. Scherble, L. Hartmann, R. Thomann, B. Ivan, R. Mülhaupt, J. C. Tiller, *Macromolecules* **2005**, *38*, 2431.

[25] T. Yoshida, A. Morinaka, *J. Photochem. Photobiol., A* **1992**, *63*, 227.

[26] A. Radu, R. Byrne, N. Alhashimy, M. Fusaro, S. Scarmagnani, D. Diamond, *J. Photochem. Photobiol., A* **2009**, *206*, 109.

[27] R. A. Evans, T. L. Hanley, M. A. Skidmore, T. P. Davis, G. K. Such, L. H. Yee, G. E. Ball, D. A. Lewis, *Nat. Mater.* **2005**, *4*, 249.

[28] B. Schmidt, P. J. Anderson, L. W. Doyle, D. Dewey, R. E. Grunau, E. V. Asztalos, P. G. Davis, W. Tin, D. Moddemann, A. Solimano, A. Ohlsson, K. J. Barrington, R. S. Roberts, C. A. P. C. Tri, *JAMA, J. Am. Med. Assoc.* **2012**, *307*, 275.

[29] B. Godin, E. Touitou, *Adv. Drug Delivery Rev.* **2007**, *59*, 1152.

[30] H. Yasuda, Ikenberr. Ld, C. E. Lamaze, *Macromol. Chem.* **1969**, *125*, 108.

[31] a) V. Klang, J. C. Schwarz, B. Lenobel, M. Nadj, J. Aubock, M. Wolzt, C. Valenta, *Eur. J. Pharm. Biopharm.* **2012**, *80*, 604; b) N. Sekkat, Y. N. Kalia, R. H. Guy, *J Pharm. Sci.* **2002**, *91*, 2376; c) M. Krulikowska, J. Arct, M. Lucova, B. Cetner, S. Majewski, *Skin Res. Technol.* **2013**, *19*, 139.

[32] N. Sekkat, Y. N. Kalia, R. H. Guy, *J. Pharm. Sci.* **2004**, *93*, 2936.

[33] S. P. Huong, H. Bun, J.-D. Fourneron, J.-P. Reynier, V. Andrieu, *Skin Res. Technol.* **2009**, *15*, 253.

[34] a) N. Sekkat, Y. N. Kalia, R. H. Guy, *Pharm. Res.* **2004**, *21*, 1390; b) S. A. Watson, G. P. Moore, *J. Anat.* **1990**, *170*, 1.